

## STUDY OF A COMMERCIAL SiO<sub>2</sub> SOL AND GEL BY SMALL ANGLE X-RAY SCATTERING: EFFECT OF SAMPLE THICKNESS AND INTERPRETATION BY MEANS OF SMOLUCHOWSKI SCHEME

YINGNIAN XU,<sup>1</sup> PANG L. HIEW,<sup>1</sup> MATTHEW AKIRA KLIPPENSTEIN,<sup>1</sup> AND YOSHIKATA KOGA<sup>2,†</sup>

<sup>1</sup> Department of Chemistry, The University of British Columbia, Vancouver, B. C., Canada V6T 1Z1

<sup>2</sup> Center for Ceramics Research, Research Laboratory of Engineering Materials, Tokyo Institute of Technology Nagatsuta, Midori-ku, Yokohama, 227 Japan

**Abstract**—Ludox HS SiO<sub>2</sub> sols at high concentrations show a peak in small angle x-ray scattering (SAXS) reminiscent to a “structure.” The appearance of such a peak was found to depend crucially on the thickness of the sample cell used for SAXS measurements. The thinner the cell used, the more prominent the peak. When the thickness was larger than 2 mm, it was no longer observable. When sols were treated with activated charcoal powders (in order to remove a surfactant) the peak became less prominent.

For the cases where clear features for structure were absent (thick sample regime), the Smoluchowski scheme was utilized to study the nature of sols. Namely, the distribution of the Smoluchowski species were estimated by numerically calculating the size distribution of particles directly from SAXS data. The distribution was found basically bimodal, and the main distribution peak, particularly for dilute sols (less than 5 wt%), was consistent with primary particles of SiO<sub>2</sub>. The second distribution peak was strongly dependent on the concentration of SiO<sub>2</sub> particles. The observed trend was that the higher the concentration of SiO<sub>2</sub> particles, the more prominent the second distribution peak and the locus of the maximum tended to move toward a smaller value in diameter. This behavior of the second distribution peak of the Smoluchowski species is no doubt a manifestation of the interparticle correlation. The observation of such behavior may provide a convenient means to characterize sols with interparticle correlation. This method was also applied for characterizing gels formed when the pH values were altered.

**Key Words**—Dependence of Sample Thickness; Ludox HS SiO<sub>2</sub>; SAXS; Smoluchowski Scheme; Structure in sol.

### INTRODUCTION

Ludox SiO<sub>2</sub> sols are used extensively in studies of colloid since they are exceptionally stable and readily available. They have almost become the standard sample against which an experimental technique is tested. For the experiment, we built a small angle x-ray scattering (SAXS) apparatus with film detection.

For the purpose of its performance test, we measured scattering from Ludox HS SiO<sub>2</sub> samples among others. In earlier studies on Ludox SiO<sub>2</sub> sols by SAXS (Shuin 1977; Matsuoka et al. 1988) and SANS, (Ramsay and Booth 1983; Ramsay et al. 1983; Penfold and Ramsay 1985; Bunce et al. 1985) broad peaks were observed in the scattering data from highly concentrated sols (about 30 to 40 wt%) with the sample cell, the thickness of which varied from 1 mm (Ramsay and Booth 1983; Ramsay et al. 1983) to 6 mm (Shuin 1977). In contrast in our study, such peaks were not observed when the thickness of the sample cell was

larger than 2 mm. However, using a 0.5 mm thick cell, we reproduced the earlier data (Shuin 1977; Matsuoka et al. 1988; Ramsay and Booth 1983; Ramsay et al. 1983; Penfold and Ramsay 1985; Bunce et al. 1985) almost completely. Artifacts are possible, but our observations appeared to be real.

In the first part of this paper, we report our observation of this unusual thickness dependence of SAXS curve from Ludox HS 40 SiO<sub>2</sub> samples. As the thickness of the sample decreases, a peak in SAXS data reminiscent to “structure” becomes more prominent. A treatment with activated charcoal, which may possibly absorb a surfactant in the sol, reduced such thickness effect. Conversely, Al<sub>2</sub>O<sub>3</sub> sols showed entirely normal thickness dependent behaviors.

In the second part, we analyzed the SAXS data by adopting the Smoluchowski scheme for the cases where the sample cells are thicker than 2 mm and there are no apparent peaks in SAXS data (thick sample regime). As described in detail below, this provided a convenient means to index inter-particle correlation hidden in SAXS data, without a detailed knowledge about the mechanisms of interparticle interactions. This method was applied for characterizing gels,

† Permanent address: Department of Chemistry, The University of British Columbia, 2036 Main Mall, Vancouver, B.C., Canada V6T 1Z1.

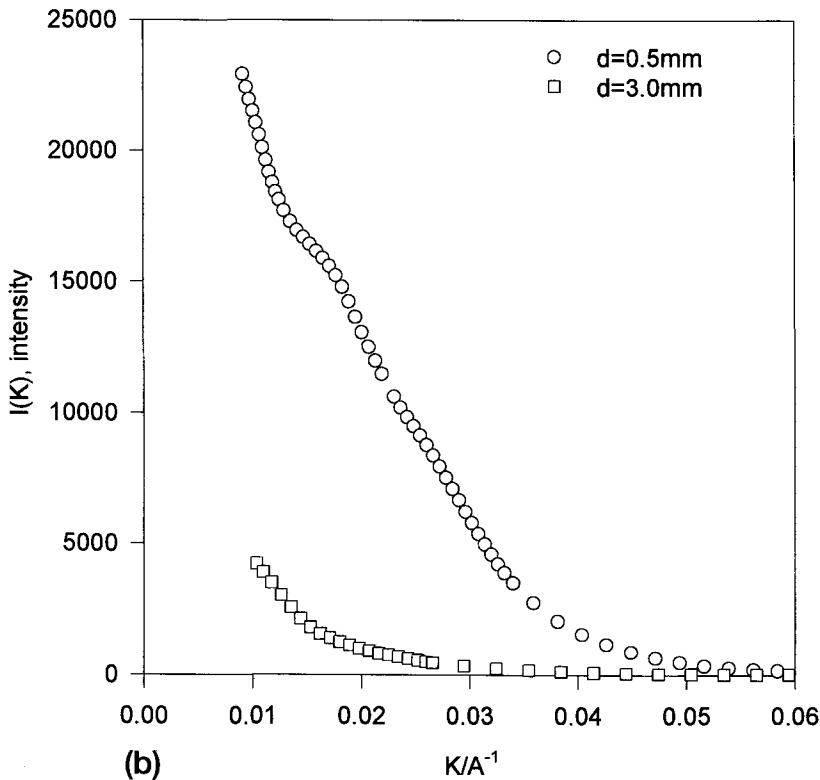
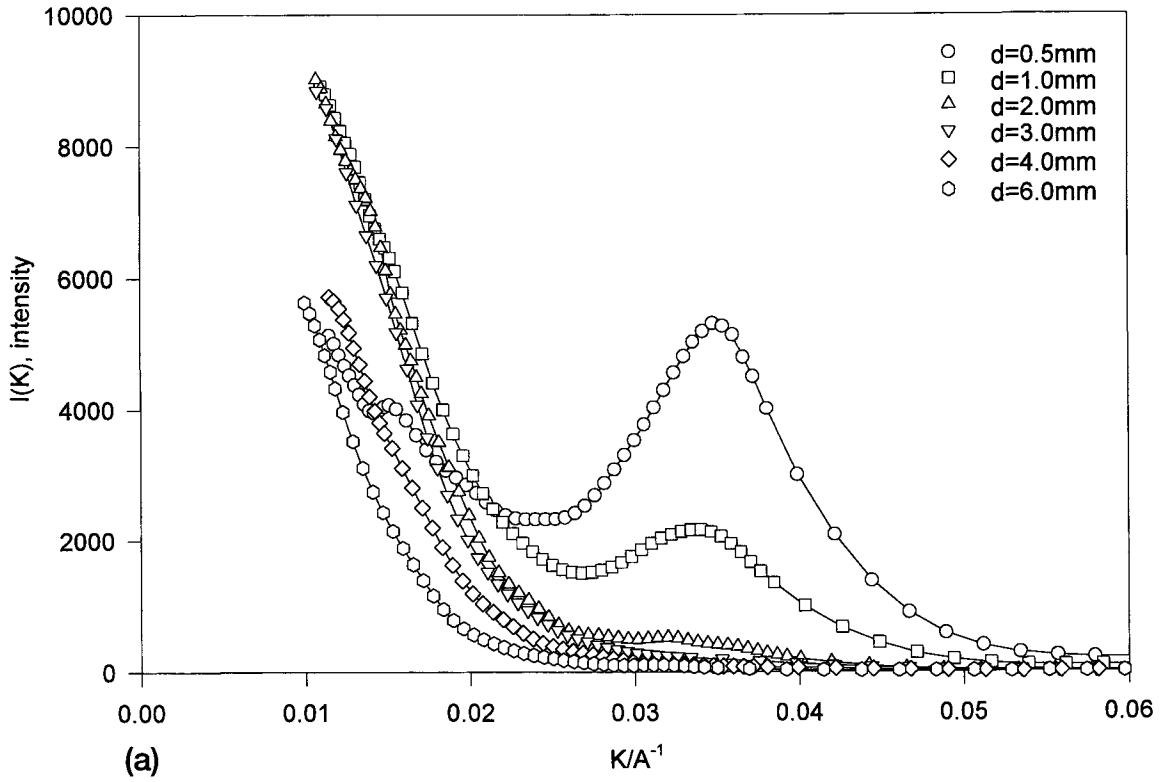


Figure 1. Effect of sample thickness on SAXS curves: (a) 40 wt% Ludox HS/91; (b) 10 wt% Ludox HS/91.

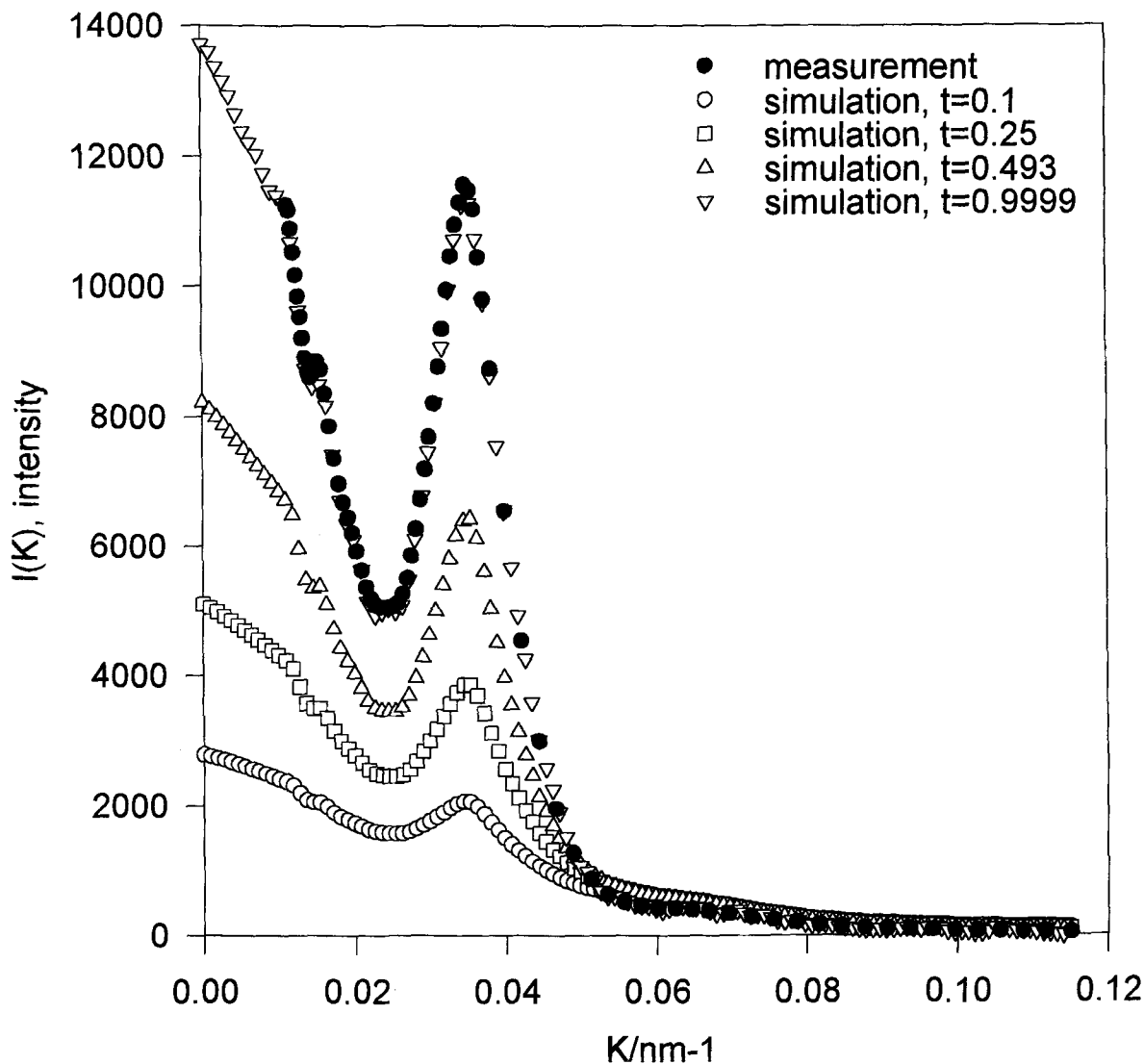


Figure 2. Effect of multiple scattering on measure data for 40 wt% with 0.5 mm cell.

which should contain highly complicated inter-particle correlation.

#### EXPERIMENT

The two specimens of Ludox HS-40 SiO<sub>2</sub> sols used were donated by Canadian Paint and Colours Ltd. We distinguish them by the year of receipt as Ludox HS/91 and Ludox HS/93. The supplier's specification relevant to the present work is: 40 wt% as SiO<sub>2</sub>, pH = 9, the average particle diameter = 120 Å. A Borax buffer of 0.01 M (pH = 9) was used to dilute sols as required. For gel formation, Ludox sols were diluted by the Borax buffer 0.01 M and then drops of 6 M HCl were added to lower the value of pH. Al<sub>2</sub>O<sub>3</sub> sol, 20 wt% colloidal dispersion in water of particle size 100 Å from Johnson Matthey, LOT # L04B08, was

used to check if the observed phenomena were specific to Ludox SiO<sub>2</sub> sols.

A Kratky camera was assembled using a Kratky slit system donated by C. G. Vonk. It was installed on a table top X-ray generator (1.5 kW) with a fine focus copper target. For detection of scattering, the film method (Vonk and Pijers 1981; Moonen 1987) was adopted. For calibration of the detecting system including a home made densitometer for digitizing a developed film, we closely followed what is described in the reference of Moonen (1987). We chose Agfa-Gavaert Structorex D7 for our film (Vonk and Pijers 1981; Vonk 1988). A piece of plastic was used as the standard sample to normalize fluctuations in X-ray intensity and conditions of developing film, etc. On the same film, three scatterings were recorded; the first

Table 1. Loci of peaks in SAXS.

Sample	Concentration (wt %)	Sample cell	Cell thickness (mm)	Locus of Max. in I $K_{max}$ ( $\text{\AA}^{-1}$ )	Locus of shoulder $K_{max}$ ( $\text{\AA}^{-1}$ )
Ludox HS/91	40	Brass/Mylar	0.5	0.036	0.015
			1.0	0.034	0.015
			2.0	0.032	0.014
			3.0	—	0.014
			4.0	—	0.014
Ludox HS/91	40	Teflon/Mylar	1.0	0.034	0.015
			3.0	—	—
			4.0	—	—
Ludox HS/91	40	Glass tube	0.5	0.034	—
			1.5	—	—
			5.0	—	—
Ludox HS/93	40	Brass/Mylar	0.5	0.035	—
			1.0	0.035	—
			3.0	—	—

from the sample, the second from the solvent and the third from this plastic standard. The sample cell was made of brass or Teflon with the nominal thickness of 0.5, 1, 2, 3, 4, or 6 mm and Mylar ( $5 \mu\text{m}$ ) windows. In addition, glass of 0.5 mm I.D. Mark capillary and 1.5 and 5 mm I.D. NMR tubes were used.

Scattering time varied from 20 min to 48 h depending on the concentration of  $\text{SiO}_2$  particles. For each sample, two sets of scattering were taken, differing in scattering time by one or two orders of magnitude. This was to improve the statistic data at larger angles where scattering intensity is very low. Two sets of data were combined to obtain scattering data in the region,  $0.01 < K < 0.22 \text{\AA}^{-1}$ ; where  $K$  is the momentum transfer for scattering and is written as:

$$K = (4\pi\sin\theta/\lambda) \quad [1]$$

$2\theta$  is the scattering angle and  $\lambda$  is the wavelength of the incident x-ray. The scattering data from the Kratky slit collimation were desmeared to obtain the scattering intensity  $I(K)$  as a function of  $K$ . For this and other data analysis, FFSAXS, a software by Vonk (1975), was used.

The performance of the SAXS system, including data analysis, was tested by measuring SAXS from a porous Vycor glass (Dow Corning, type 7930) in a 0.5 mm cell. The average pore diameter of this specimen had been previously determined by a variety of techniques (Handa et al. 1992). The pore size distribution determined by our SAXS measurement system showed a monodispersed distribution that peaked at exactly the same diameter.

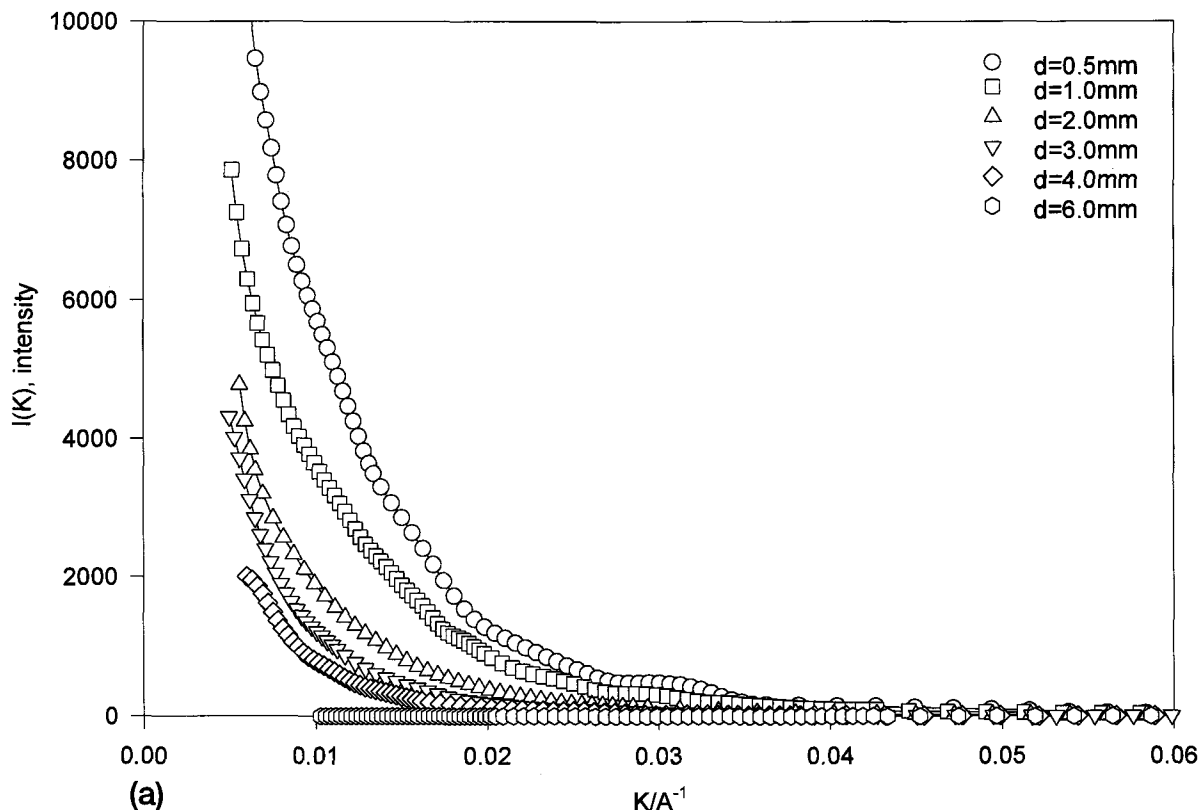


Figure 3. Effect of sample thickness on SAXS intensity: (a) 10 wt%  $\text{Al}_2\text{O}_3$  sol; (b)  $\text{Al}_2\text{O}_3$  sol, 10 wt%; (c) Ludox HS/91, 40 wt%.

## RESULTS AND DISCUSSION

## Thickness Dependence of "Structure" (thin sample regime)

Figure 1a shows the desmeared scattering intensity  $I(K)$  for Ludox HS/91, the undiluted (40 wt%) sample, and Figure 1b the 10 wt% sample, using cells made of brass with various thickness. Multiple scattering may be present for a thicker sample (Schelten and Schmatz 1980; Monkenbusch 1991). The analytically explicit expression for multiple scattering was derived and applied for small angle neutron scattering (SANS) data from voids in metals sample (Schelten and

Schmatz 1980). It was shown that the apparent radius of gyration due to multiple scattering diminished to about  $1/3$  and the Porod constant increased in turn by a factor of about 1.5 (Schelten and Schmatz 1980), but there never was a qualitative change in the shape of the scattering curve, or the appearance/disappearance of any "peak." When applied for SANS data from an AOT, asodium 1, 4-bis(2-ethylhexyl)sulfosuccinate microemulsion, which showed a clear peak, the latter did not exhibit any change in shape or locus of the maximum (Monkenbusch 1991). To calculate the effect of multiple scattering explicitly, the software "MUX DEMOX" software by Monkenbusch (1991) was applied to the scattering data for 40 wt% silica sol of 0.5 mm thick, the scattering with a clear peak. The parameter used in this software is the transmission value rather than the sample thickness. As the sample thickness increased from 0.5 mm to 6 mm, the transmission of 40 wt% silica sol decreased to 0.25. Thus, the scattering data for 40 wt% silica sol with a 0.5 mm sample cell were used as the input data and those after multiple scattering were calculated with varying value of transmission,  $t$ . Figure 2 shows the results. The fact that the scattering for  $t = 0.9999$  recovered the input data completely assured the health of numerical integration of the software. As exhibited in the figure, the effect of multiple scattering, aside from the decrease in transmission, does not alter the locus of the maximum although the peak appears to broaden. Therefore, the thickness dependent behavior in Figures 1a and 1b is not due to multiple scattering.

We repeated the measurements with Teflon cells of thickness, 1, 3, 4, and 6 mm, and used glass tubes of inner diameter, 0.5, 1.5 and 5 mm. For all of the cases, the trend is similar. Table 1 lists the loci of the peaks. The "—" mark in the table distinguishes no peak was observed. Thus, the observed thickness dependence is not due to material used for the cell.

To check possible artifacts associated with the apparatus, Al<sub>2</sub>O<sub>3</sub> sol (10 wt%) was measured using the brass cells with varying thickness. As shown in Figure 3a, the SAXS data showed a normal thickness dependent behavior. Ignoring multiple scattering, the intensity  $I$  can be written as:

$$I \propto d \exp(-\mu d) \quad [2]$$

where  $d$  is the thickness and  $\mu$  is the absorptivity of the sample. Therefore, at a fixed value of  $K$ , the quantity,  $\{\ln(I) - \ln(d)\}$ , should be linear to  $d$  and the slope,  $-\mu$ , should not depend on  $K$ . Figure 3b indicates that is indeed the case for an Al<sub>2</sub>O<sub>3</sub> sol, considering uncertainty in  $d$ . For comparison, see Figure 3c for Ludox HS/91 (40 wt%). Thus, we conclude that the thickness dependent behavior shown in Figure 1a is specific to Ludox HS SiO<sub>2</sub> sols and not due to an artifact associated with the apparatus.

Figure 4 shows the dependence of SAXS data on

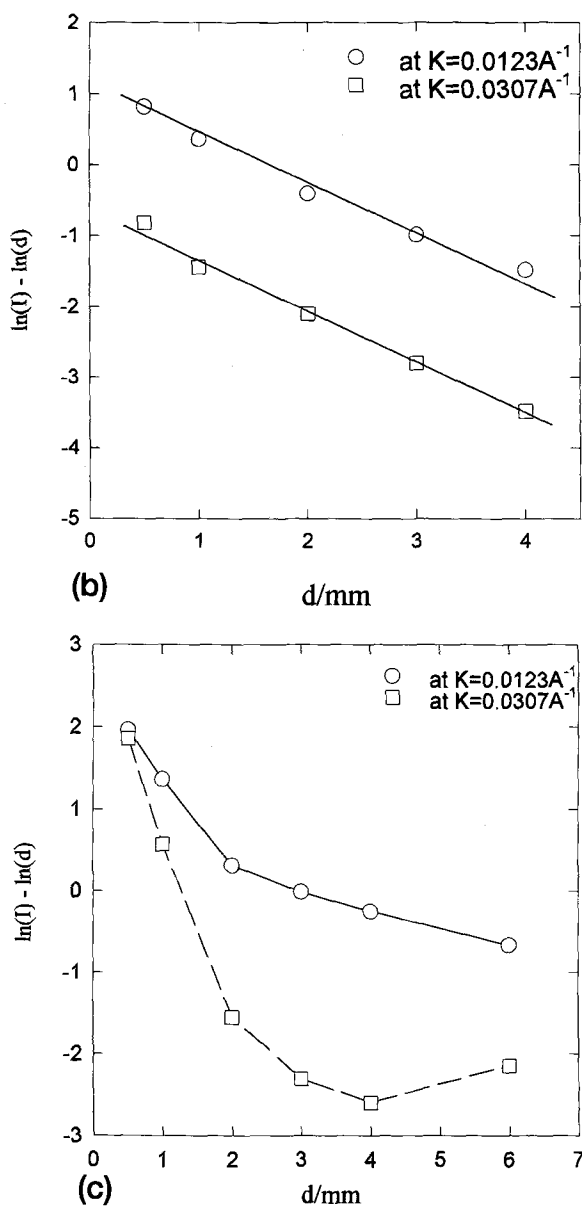


Figure 3. Continued.

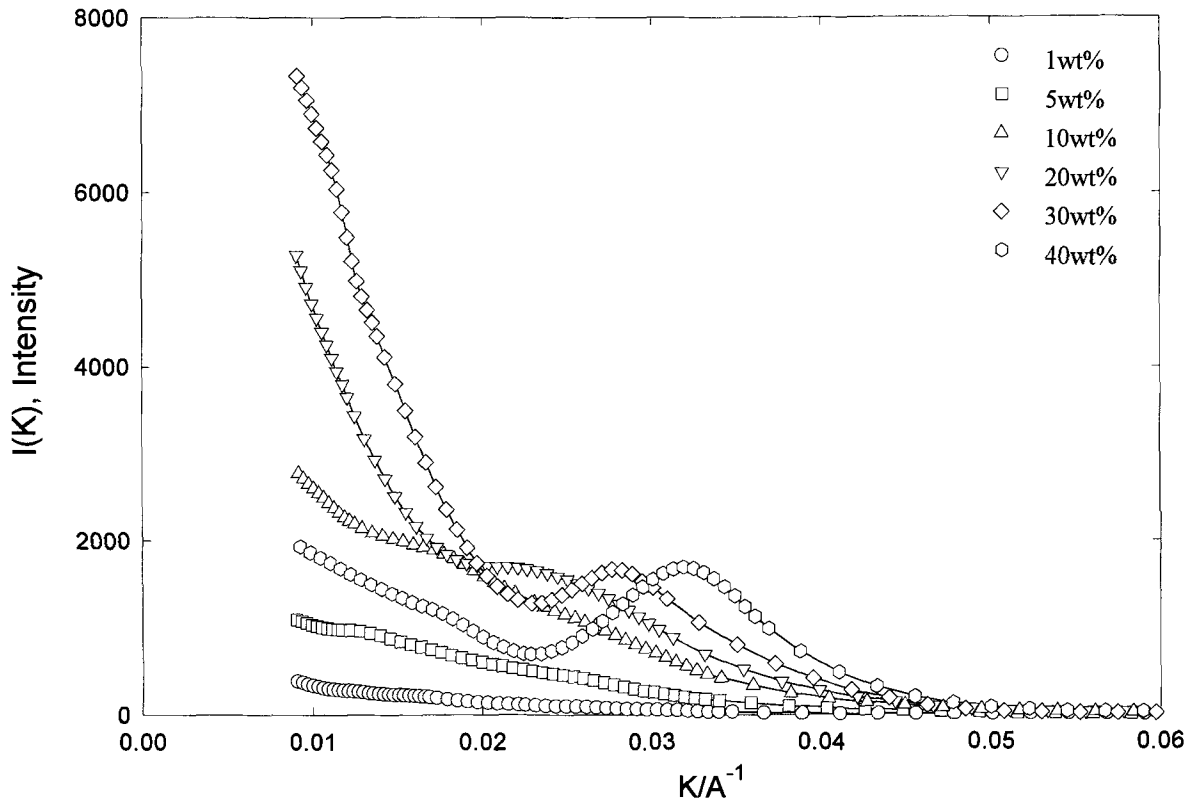


Figure 4. SAXS intensity curves,  $I(K)$ , of Ludox HS/93 with 0.5 mm sample cell at various concentrations of  $\text{SiO}_2$  particles.

the concentration of Ludox HS/93 measured using a 0.5 mm brass cell. An earlier SAXS study on Ludox HS  $\text{SiO}_2$  sols (Shuin 1977), whereby the cell used was 6 mm thick with Mylar ( $5 \mu\text{m}$ ) windows, showed a similar concentration dependence to our data using a 0.5 mm cell. Another SAXS study on Ludox SM dialyzed against  $10^{-4}$  M NaOH using 1.5 mm I.D. glass capillary suggested an ordered structure from a peak in a SAXS curve for higher  $\text{SiO}_2$  and lower electrolyte concentrations (Matsuoka et al. 1988). SANS studies on Ludox HS using a 1 or 2 mm quartz cell also indicated similar behaviors (Ramsay and Booth 1983; Ramsay et al. 1983; Penfold and Ramsay 1985; Bunce and Ramsay 1985). Table 2 summarizes the loci of peaks of the above scattering data. For Ludox HS samples, the loci of peaks concur with our data using 0.5 mm cells and those in literature using 1 to 6 mm sample cells.

Such peaks in  $I(K)$  were interpreted in two different ways. One approach is to regard sol as liquid-like. The structure factor  $S(K)$  calculated using a model in which the pair potential is approximated as a hard core with a soft tail was fitted to that observed (Ramsay and Booth 1983; Ramsay et al. 1983; Penfold and Ramsay 1985; Bunce and Ramsay 1985). A soft tail is to model the screened coulombic repulsion between charged particles. The fit was successful for the case where the values of surface charges are markedly less

than those previously reported. The actual repulsion among particles is drastically more suppressed than expected from the surface charges alone.

Another interpretation is to regard sol as having an ordered crystalline-like structure with distortion (Matsuoka et al. 1987). In this approach, a peak in  $I(K)$  is the first order Bragg diffraction with higher order peaks diminishing due to "paracrystalline" distortion (Matsuoka et al. 1987). The spacing of this ordered structure was found to be much smaller than the case in which particles are distributed randomly. The latter case has been normally expected from the electrostatic repulsion alone due to surface charges (Matsuoka et al. 1988). The  $\text{SiO}_2$  particles therefore attract each other by this interpretation (Matsuoka et al. 1987). Since our data with a 0.5 mm cell are almost identical with those observed in the above investigations, either interpretation can be applicable. Whichever interpretation might be closer to reality, both indicate that  $\text{SiO}_2$  particles attract each other and the inter-particle distance decreases on increasing the particle concentration. Indeed, recent theoretical works taking into account the many-body nature of the problem suggest attraction among particles with the same charge (Sogami and Ise 1984; Groot 1990, 1991; Valteau et al. 1991).

In passing, some comments are in order regarding

Table 2. Loci of peaks in SAXS or SANS.

Sample	Concentration	Method	Sample cell	Locus of Max. in I $K_{max} (\text{Å}^{-1})$	References
Ludox HS/93	40 wt %	SAXS	0.5 mm	0.033	Fig. 4, this work
	30 wt %	SAXS	0.5 mm	0.028	
	20 wt %	SAXS	0.5 mm	0.023	
	10 wt %	SAXS	0.5 mm	0.018	
Ludox HS/91	40 wt %	SAXS	0.5 mm	0.035	
	30 wt %	SAXS	0.5 mm	0.030	
	10 wt %	SAXS	0.5 mm	0.019	
Ludox HS	30 wt %	SAXS	6 mm	0.028	Shuin 1977
	20 wt %	SAXS	6 mm	0.025	
	10 wt %	SAXS	6 mm	0.019	
Ludox SM	30 wt %	SAXS	6 mm	0.031	
	20 wt %	SAXS	6 mm	0.022	
	10 wt %	SAXS	6 mm	0.019	
Ludox SM	16.98 Vol%	SAXS	1.5 mm $\phi$ capillary	0.0333	Matsuoka 1988
	5.49 Vol%	SAXS		0.0269	
Dialyzed against $10^{-4}$ M NaOH	3.66 Vol%	SAXS		0.0237	
	2.75 Vol%	SAXS		0.0226	
Ludox HS	0.65 g/cm <sup>3</sup>	SANS	1 mm or 2 mm quartz cell	0.033	Ramsay et al. 1983
	0.41 g/cm <sup>3</sup>	SANS		0.030	
	0.16 g/cm <sup>3</sup>	SANS		0.018	

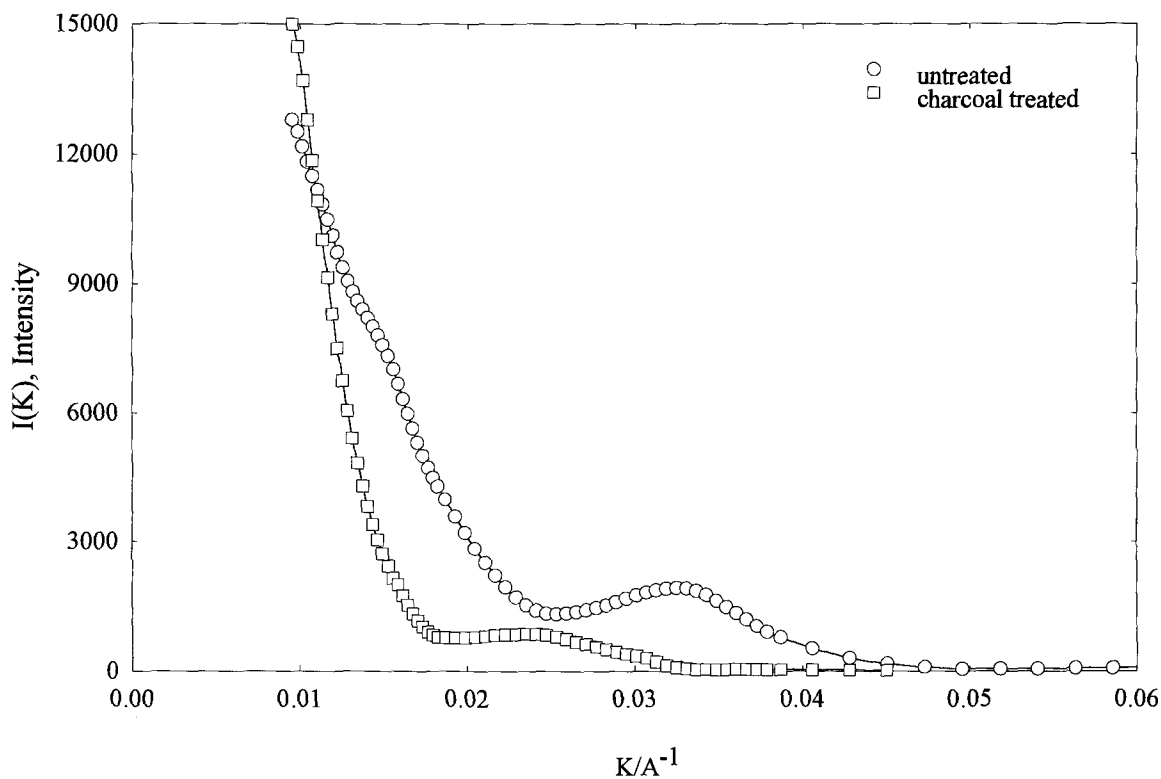


Figure 5. Effect of charcoal treatment on SAXS intensity curve of Ludox HS/93, 40 wt%.

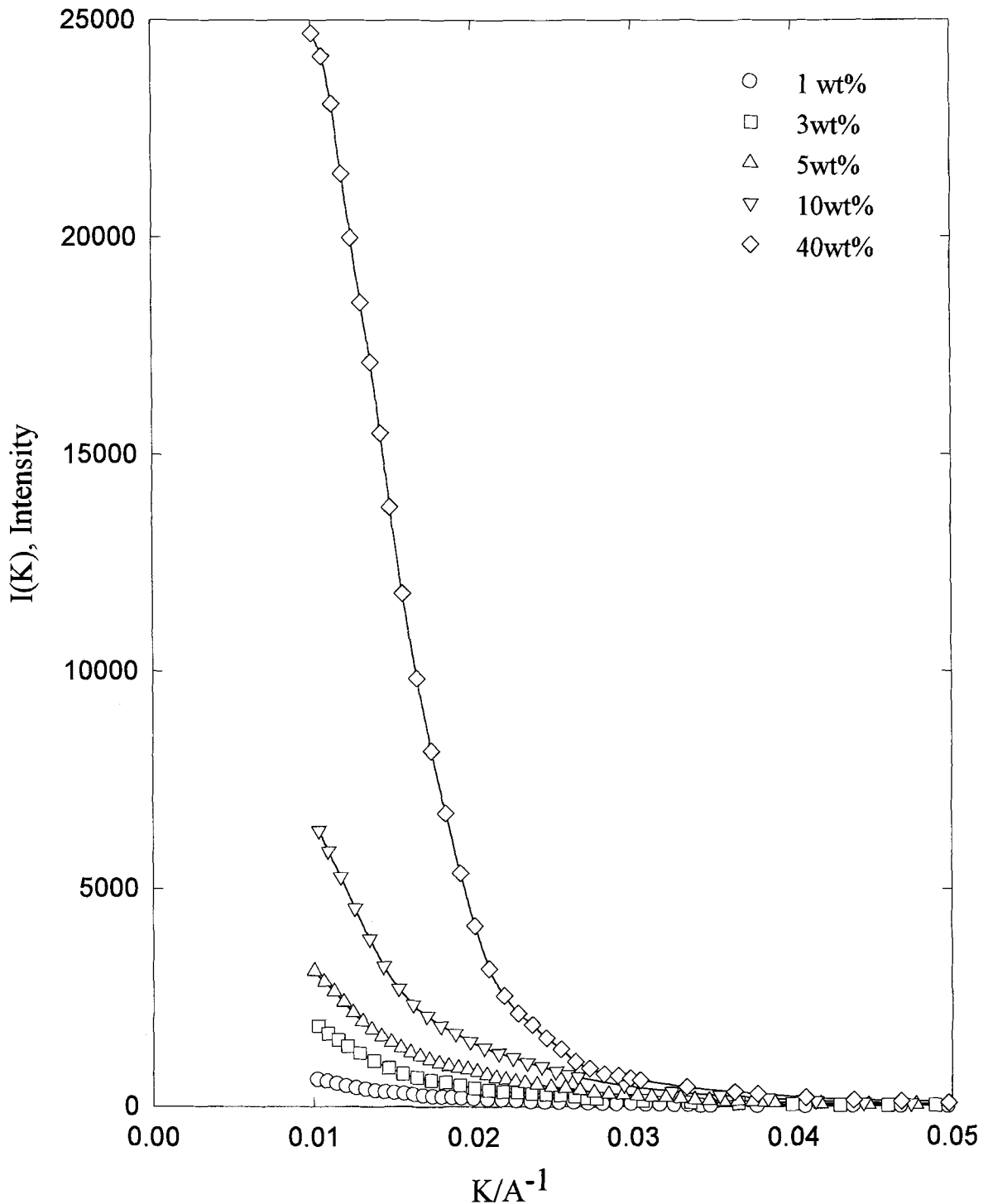


Figure 6. SAXS intensity curves,  $I(K)$ , of Ludox HS/91 with 3 mm sample cell at various concentrations of  $\text{SiO}_2$  particles.

determination of  $S(K)$  from experimental data  $I(K)$ . It is customary to *assume* that when the particle concentration is low, there is no interparticle correlation, that is  $S(K) \approx 1$ . Thus  $I(K)$  is written as:

$$I(K) = I_e n_p (\rho_1 - \rho_2)^2 V_p^2 P(K) S(K) \quad [3]$$

where  $I_e$  is the intensity scattered by one electron,  $n_p$  is the density number of particles,  $\rho_1$ ,  $\rho_2$  are the elec-



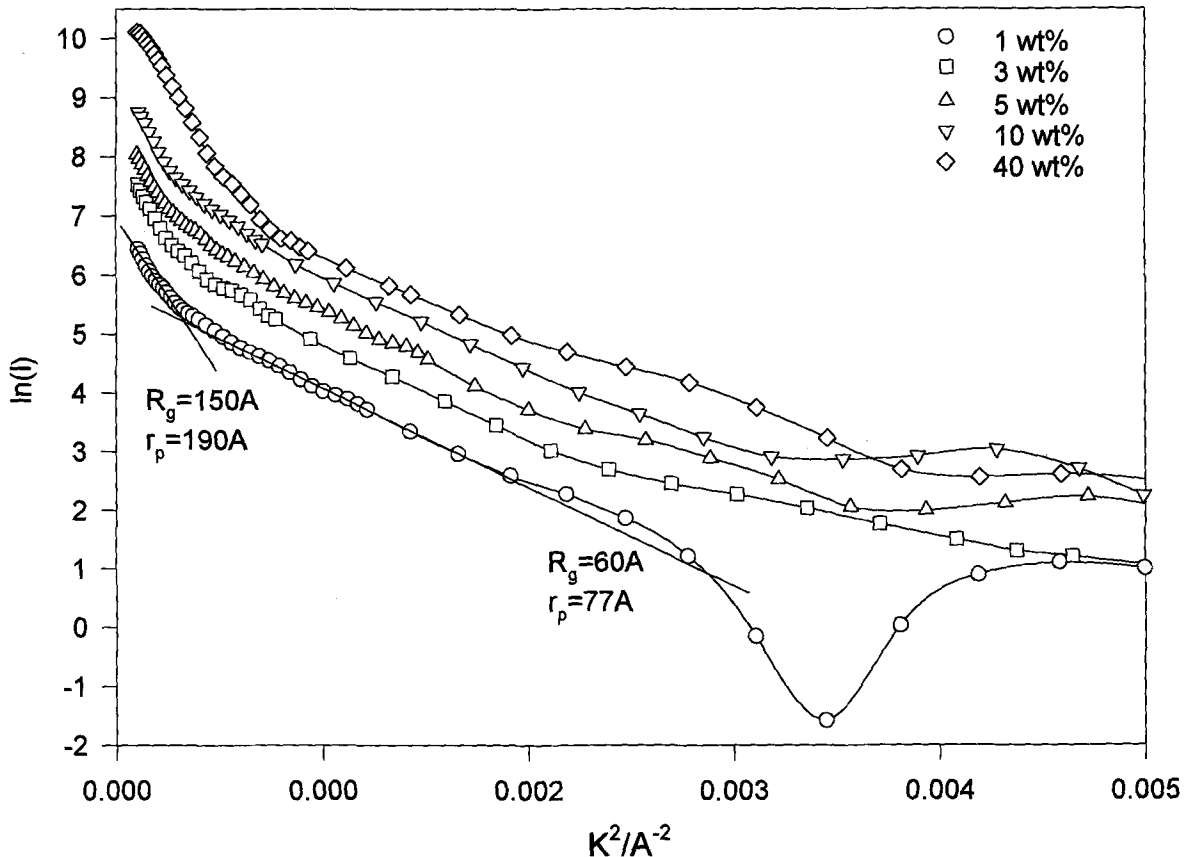


Figure 7. Guinier plots for Ludox HS/91 with 3 mm sample cell at various concentrations.

tron densities of the particle and the suspending medium,  $V_p$  is the volume of the particles, and  $P(K)$  is called the form factor showing scattering from an isolated particle. For the limit of  $n_p \rightarrow 0$ ,  $S(K) \rightarrow 1$ , then:

$$I(K)_{n_p \rightarrow 0} = I_c n_p (\rho_1 - \rho_2)^2 V_p^2 P(K) \quad [4]$$

For a previous SANS work (Ramsay et al. 1983), the data from the most dilute sample, 0.020 g/cm<sup>3</sup>, was used as  $P(K)$ . In a work by SAXS (Matsuoka et al. 1988), the data from a 5.5 vol% with 0.1 M NaCl sample was used for  $P(K)$ . When the data from the latter was compared with those from a 0.11 vol% sol with no electrolyte, it successfully tested the assumption of  $S(K) \approx 1$ . It is puzzling in the light of a work by Allen and Matijevic (Allen and Matijevic 1969) in which it was concluded that at high electrolyte concentration, SiO<sub>2</sub> particles tend to coagulate. Indeed, the condition (10<sup>-4</sup> M NaOH, 0.1 M NaCl) is very close to the coagulation boundary. In any case, it should be pointed out that an absolutely unequivocal estimation of  $P(K)$  for a real, not quite monodispersed, sol has never been established in the works of SAXS and SANS. In light scattering, sols must be diluted to less than 10<sup>-4</sup> wt% for  $S(K) \approx 1$  (Xu et al. 1994b, personal communication).

#### Thickness dependence

The question remains as to why the peak in our data of  $I(K)$  diminishes when the thickness of a sample is increased to more than 2 mm. We recall recent works by Wasan et al. (1992; Nikolov and Wasan 1992) in which structural formation of SiO<sub>2</sub> particles in Ludox HS is probed by stratification of thin films of the sol. Their findings may be summarized as follows:

- (1) Thin films of sol are stabilized by "crystallization" of colloidal particles.
- (2) The more concentrated the SiO<sub>2</sub> particles are and the smaller the diameter of film, a larger number of SiO<sub>2</sub> particle layers form a crystal-like structure.
- (3) For 190 Å SiO<sub>2</sub> particles, 20 vol% (30 wt%) and the film diameter of less than 0.6 mm, three SiO<sub>2</sub> particle layers are stabilized in a horizontal film.
- (4) If a surfactant is present, the film of a larger number of layers is stabilized. This was tested by first removing a surfactant from Ludox HS sol by a charcoal treatment.

Their findings of (2) and (3) may have some con-

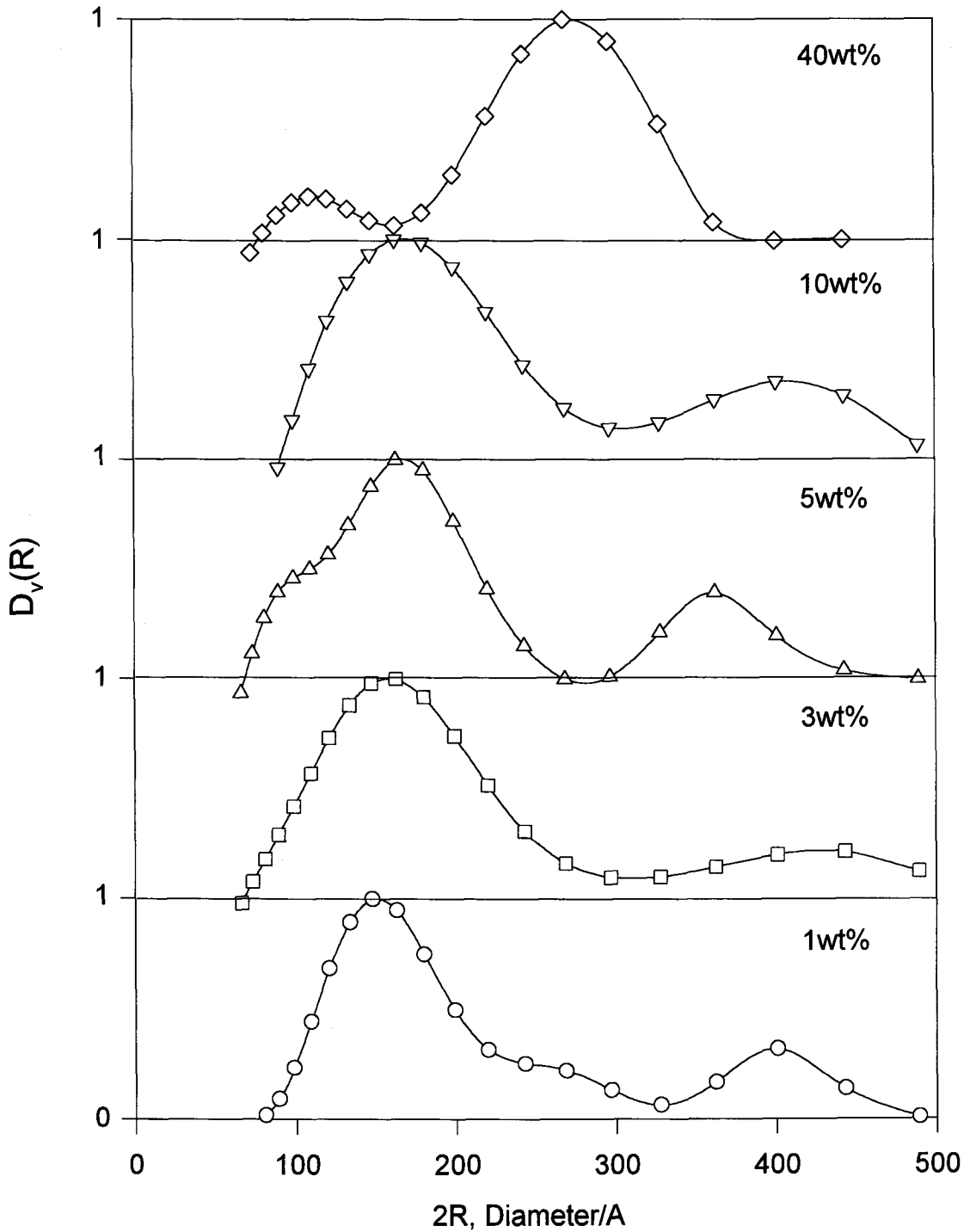


Figure 8. Size distribution of Ludox HS/91 with 3 mm sample cell at various concentrations.

nection to what we observed. Figure 5 shows  $I(K)$  from Ludox HS/93 samples with a 1 mm cell before and after treatment by activated charcoal following the procedure described by Nikolov and Wasan (1992). It

is apparent that a possible removal of a surfactant from the present Ludox HS/93 sol decreases the tendency of structure enhancement, along the line of conclusion (4) (Nikolov and Wasan 1992).

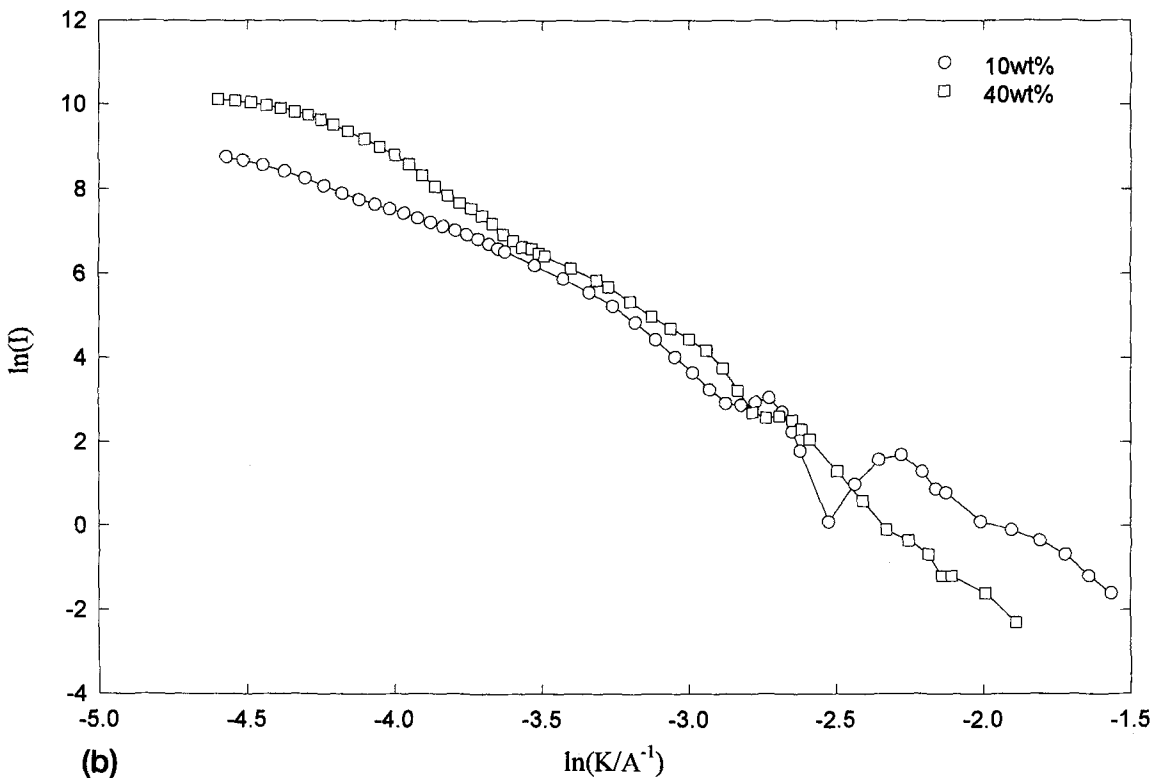
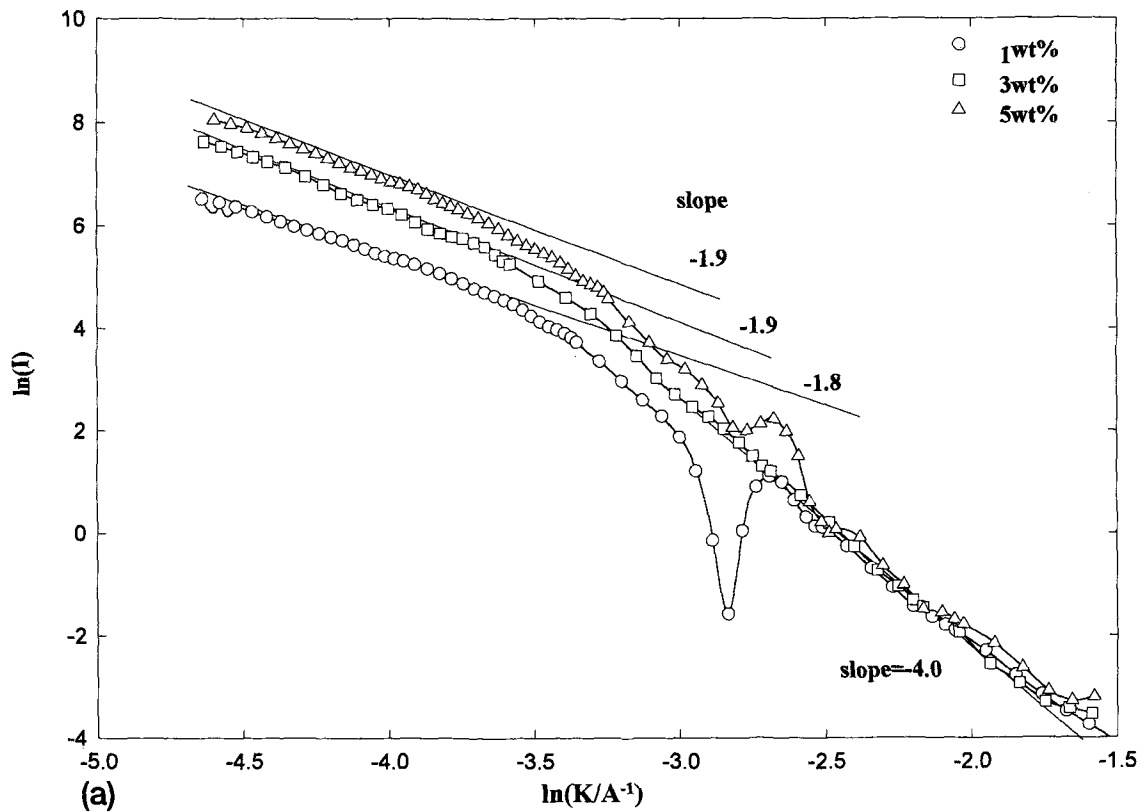


Figure 9. Log-log plot of SAXS data for Ludox HS/91 with 3 mm sample cell at various concentrations.

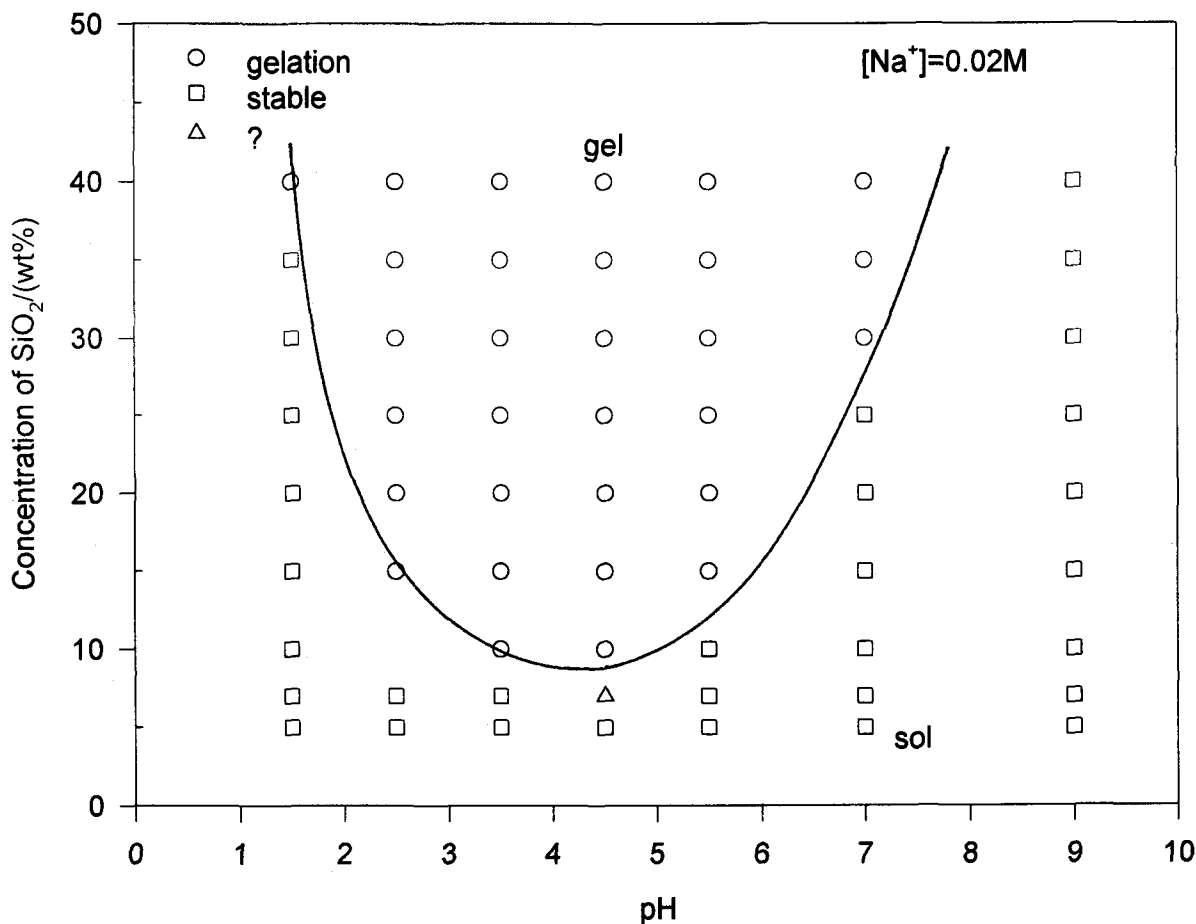


Figure 10. Gel-sol diagram for Ludox HS/91.

### Thick Sample Regime

Figure 6 shows  $I(K)$  from Ludox HS/91 using a 3 mm Teflon cell. There are no apparent features in  $I(K)$ , hence in  $S(K)$ , (if  $S(K)$  can be accurately extracted at all), or a repeat distance cannot be calculated in the "paracrystalline" approach (Matsuoka et al. 1987). Nevertheless, we wish to make an attempt to obtain as much information as possible from structureless scattering data shown in Figure 6 using the Smoluchowski scheme (Everett 1989; Brinker and Scherer 1990). It could be worthwhile to devise a method of characterization using such structureless scattering data, which are most common in real situations.

In  $I(K)$  shown in Figure 6, a constant background had been subtracted by assuming the Porod law in the range,  $0.075 < K < 0.22 \text{ \AA}^{-1}$ . The Guinier plots are shown in Figure 7. Two straight lines are apparent even for a 1 wt% sample. The straight line with the smaller slope in the range,  $0.0005 < K^2 < 0.0015 \text{ \AA}^{-2}$  gives  $R_g = 60 \text{ \AA}$  ( $R_g K < 2$ ) or  $r_p = 77 \text{ \AA}$ , where  $R_g$  is the radii of gyration and  $r_p$  represents the spherical particle. This appears reasonable in comparison with

the value of the particle diameter specified by the supplier,  $120 \text{ \AA}$ . While the apparent dip in  $\ln(I)$  at about  $K^2 = 0.0035$  may be subject to a large error, the fact that the product  $r_p K = 4.5$  at the dip may hint that the 1 wt% sample is reasonably mono-dispersed (Zerrouk et al. 1990). In spite of this, there is another apparent Guinier line with  $R_g = 150 \text{ \AA}$ , in the range  $K^2 < 0.0002$  ( $R_g K < 1.7$ ). Thus, there is another species with the diameter  $380 \text{ \AA}$ . This behavior of having two Guinier lines is common in the case with a bimodal distribution in particle size (Xu et al. 1994a; Guinier and Fournet 1955).

The size distribution may be numerically calculated in the dilute limit, that is  $S(K) \approx 1$ , by Vonk's method (1976) as:

$$I(K) = I_e(\rho_1 - \rho_2) \int_0^\infty D_v(R) V_p P(K, R) dR \quad [5]$$

where  $D_v(R) dR$  is the volume distribution of particle radius from  $R$  to  $R + dR$ . From the SAXS data shown in Figure 6, the size distributions were numerically cal-

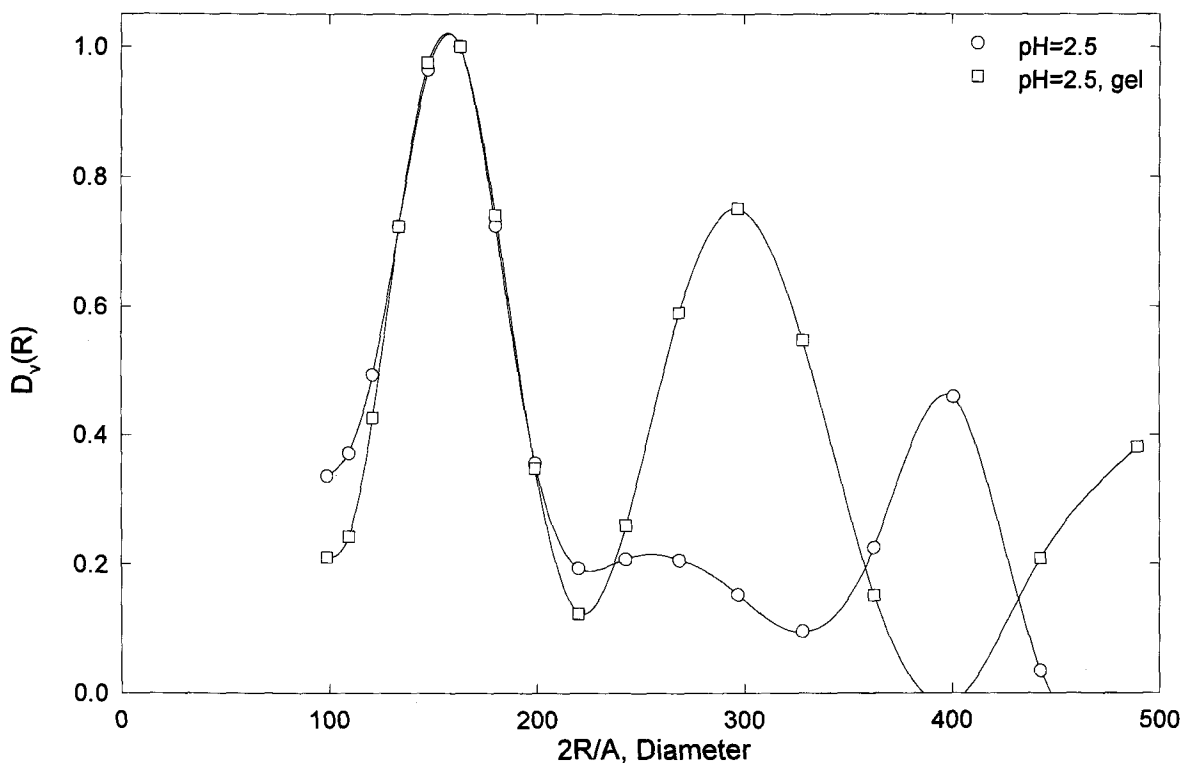


Figure 11a. Size distributions of Ludox HS/91, 10 wt%, with 3 mm sample cell, before and after gel formation of pH = 2.5.

culated by assuming particles are all spherical in shape. The resulting distributions are shown in Figure 8.

A transmission electron microscopy photograph taken by us as well as that in a previous paper (Shuin 1977) indicated Ludox HS SiO<sub>2</sub> sols consisted of reasonably mono-dispersed spherical particles. Hence, if 1% is dilute enough for losing interparticle correlation completely, then there should be only one straight line in Guinier plots, and the size distribution calculated from SAXS data should show a single narrow distribution peak centered at the average diameter of particles. Therefore, we suggest the second distribution peak at about 400 Å for 1 wt% sample is a manifestation of interparticle correlation. Thus, 1 wt% is not dilute enough for Ludox HS SiO<sub>2</sub> sols to be completely free from interparticle correlation. For the cases where I(K) exhibits a peak as our thin sample regime or in previous papers (Shuin 1977; Matsuoka et al. 1988; Ramsay and Booth 1983; Ramsay et al. 1983; Penfold and Ramsay 1985; Bunce et al. 1985), an approximate form of P(K) is all that is required to extract a reasonable form of S(K) for discussion. However, such structureless SAXS data, as shown in Figure 6, do need a very accurate form of P(K) in order for S(K) to be evaluated accurately, so that slight variations of S(K) from unity can be utilized for discussion.

In the absence of an accurate form of P(K) to evaluate S(K) with confidence, and in the absence of a

peak in I(K) that would allow the "paracrystalline" approach (Matsuoka et al. 1987), we proceeded as follows. In the so-called Smoluchowski scheme (Everett 1989; Brinker and Scherer 1990), particles in sol are taken to coagulate into dimers, trimers, tetramers, . . . etc., due to interparticle correlation, and it is assumed that once these polymers are formed they are free from inter-polymer interactions. Then the size distributions numerically calculated directly from I(K) can now be taken to show the size distribution of such Smoluchowski species. This approach in no way supports nor confirms the existence of such species. Rather, it is a convenient way to rewrite I(K) in the form of D<sub>v</sub>(R) through numerical inversion of Equation [5], so that a subtle variation in I(K) due to interparticle correlation may be magnified in the form of D<sub>v</sub>(R). Thanks to the Smoluchowski scheme, D<sub>v</sub>(R) has a convenient basis of interpretation. We recall a similar approach in the field of solution thermodynamics, whereby intermolecular interactions in solutions are understood to cause "associated" species among solute and solvent molecules (Barta et al. 1989; Dethelfson et al. 1984; Bhatia 1984; Franks and Desnoyers 1985; Costas and Patterson 1985).

In the spirit of this approach, the second distribution peak at about 400 Å may now be looked upon as an aggregated species. The log-log plots for 1 wt% sample shown in Figure 9a indicates the power law rela-

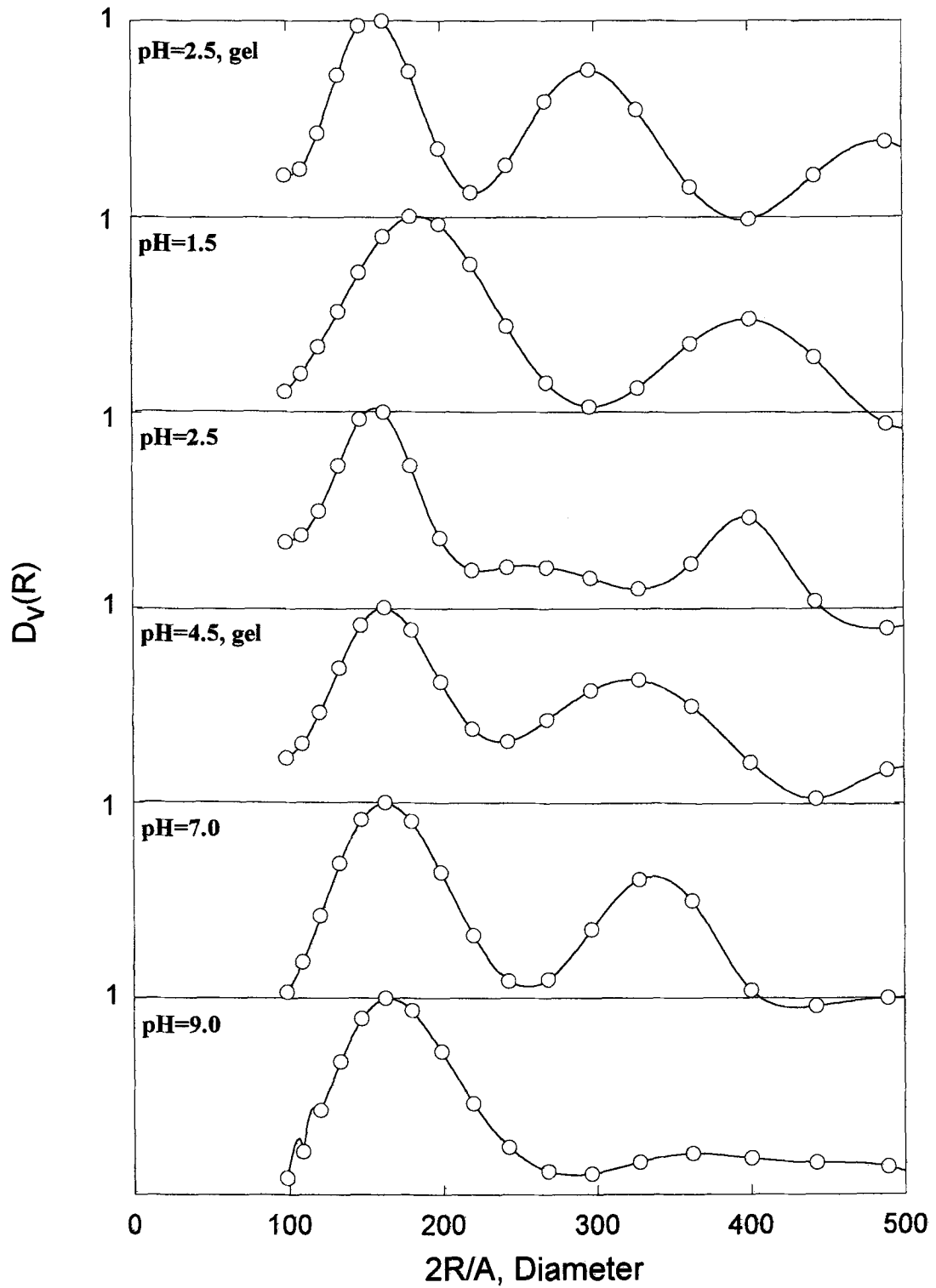


Figure 11b. Size distribution of Ludox HS/91, 10 wt%, with 3 mm sample cell, and the effect of pH.

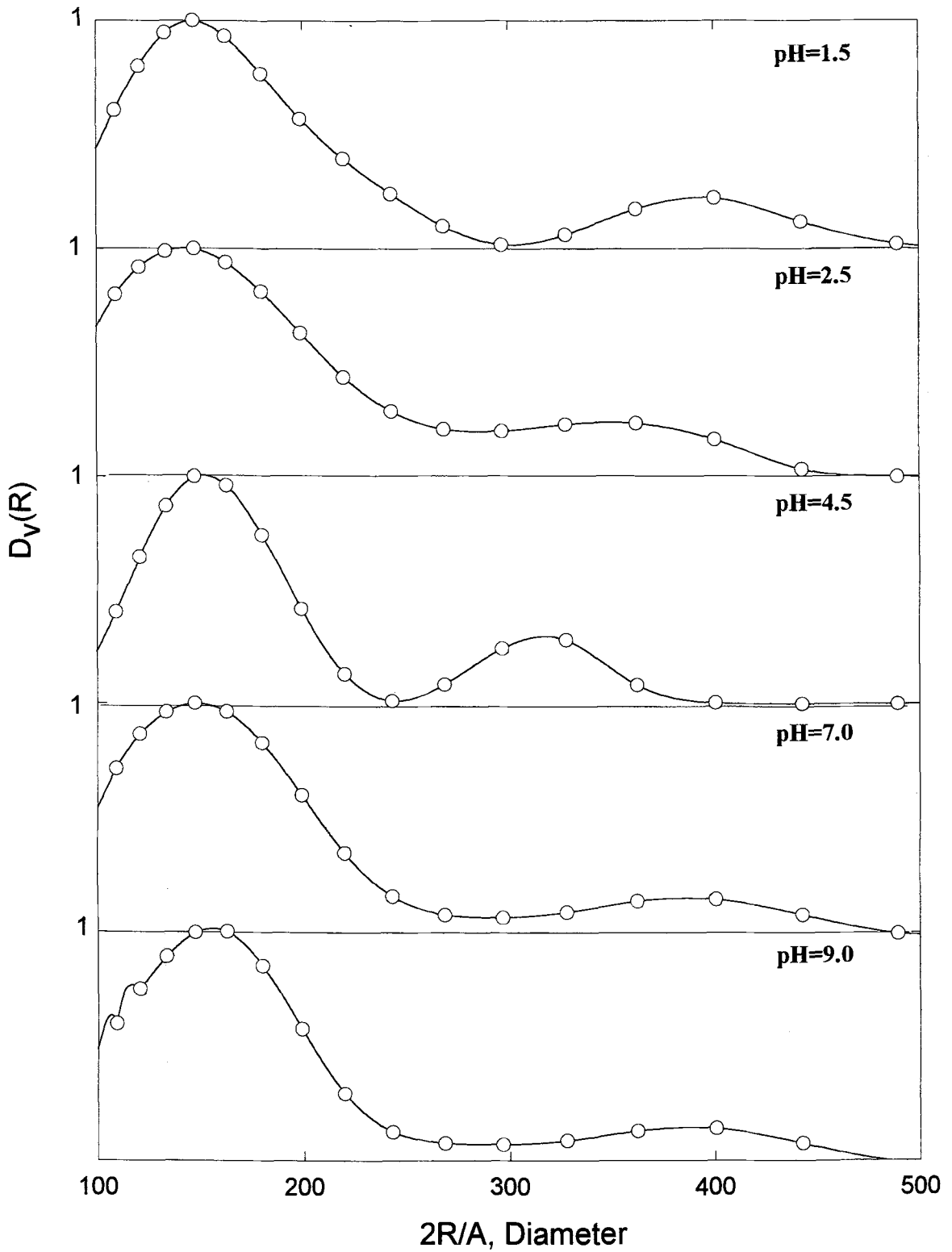


Figure 12. Size distributions of Ludox HS/91, 1 wt%, with 3 mm sample cell, and the effect of pH.

tion in the range,  $0.008 < K < 0.02 \text{ \AA}^{-1}$ , with slope  $-1.8$ . This fact hints that there are aggregates of fractal dimension 1.8 (Schaefer et al. 1984) with the monomer diameter of about  $100 \text{ \AA}$  (calculated from the upper limit value of  $K$  of the straight line in Figure 9a) and that of the aggregates of about  $300 \text{ \AA}$  (from the lower limit). Both sizes are not inconsistent with information contained in  $D_v(R)$ , Figure 8. For 3 and 5 wt% samples, the power law scatterings are still evident with the similar values of slope, as shown in Figure 9a. For 10 and 40 wt% samples, no power law is apparent, as shown in Figure 9b, that is interparticle interaction becomes more complicated. The behavior of  $D_v(R)$  shown in Figure 8 suggests that aggregation advanced in increasing the concentration. The first distribution peak widened toward larger diameters, thus the population of larger Smoluchowski species increases, as the concentration increases from 1 to 10 wt%. For the 40 wt% sample, the degree of coagulation causes a main distribution peak to shift to  $270 \text{ \AA}$ . The fact that a small peak remains at  $120 \text{ \AA}$  suggests the average diameter of primary particles is still  $120 \text{ \AA}$ . A shoulder at about  $100 \text{ \AA}$  for the 5 wt% sample supports this. However, for 10 wt%, such a shoulder is not visible. This in turn suggests that even for the 1 wt% sample there are aggregates of size a little larger than the primary particles of  $120 \text{ \AA}$  and that the apparent first distribution peak is the result of convolution of the primary particles and small size aggregates. Another feature evident from Figure 8 is that the second distribution peak generally shifts toward a smaller size during increasing concentration. Therefore, the size of aggregates shrink on increasing particle concentration. Thus, we suggest that  $\text{SiO}_2$  particles interact with each other in such a way as to form aggregates, or to attract each other in spite of surface negative charges at  $\text{pH} = 9$ . By increasing the concentration of  $\text{SiO}_2$  particles, attraction becomes stronger.

#### Application to Gel-Thick Sample Regime

By changing the value of  $\text{pH}$ ,  $\text{SiO}_2$  sols become unstable and gels form. Figure 10 is a sol/gel diagram depicting the region in the  $\text{pH}$ -concentration field, where gelation occurs. In this series of experiments, the total  $\text{Na}^+$  concentration was kept at  $0.02 \text{ M}$  and  $\text{pH}$  values were reduced by adding a very small amount of  $6 \text{ M HCl}$ . As  $\text{HCl}$  was added, the borate ions,  $\text{B}_4\text{O}_7^{2-}$  were replaced by  $2 \text{ Cl}^-$  and were converted to  $\text{H}_2\text{B}_4\text{O}_7$ , or technically  $4\text{H}_3\text{BO}_3$  with additional  $5\text{H}_2\text{O}$ . Therefore, the total ionic strength was virtually unchanged. According to Allen and Matijevic (1969),  $\text{SiO}_2$  sols coagulate when  $\text{pH} > 14$  with  $[\text{Na}^+] = 0.02 \text{ M}$  for sols of  $\text{SiO}_2$  concentration about 2 wt%. Thus, the gelation region shown in Figure 10 is not triggered by destabilization due to adsorption of  $\text{Na}^+$  ions on  $\text{SiO}_2$  surfaces (Allen and Matijevic 1969). We

checked the surface charges at 5 wt% by means of moving boundary electrophoresis and confirmed that the point of zero charge occurs at  $\text{pH} = 2.5$ . In the almost entire  $\text{pH}$  range in Figure 9, the surface charge remains negative, hinting the gelation was not due to zero surface charge.

Whatever the mechanism of the gelation may be, we study structure of gels by SAXS in the thick sample regime. Figure 11 shows the size distribution calculated from SAXS data for the 10 wt% samples, using a 3 mm cell. There were no apparent peaks in  $I(K)$ , that is in the thick sample regime. At  $\text{pH} = 2.5$ , the sol was stable for a week and then turned into gel. Figure 11a shows the size distributions of Smoluchowski species for both situations. Judging from the shift of the second distribution peak the figure suggests that on gelation the size of aggregates shrink, which is consistent with an earlier observation by TEM (Zerrouk et al. 1990). Figure 11b indicates the locus of the second distribution peak shifts to a smaller size when the value of  $\text{pH}$  decreases from 9 to 4.5 (gel) and 2.5 (gel) thereupon shifting back to a larger size, suggesting interparticle correlation is the strongest at  $\text{pH} = 2.5\text{--}4.5$ , which is consistent with gel formation in this  $\text{pH}$  range. Figure 12 shows the similar behavior for the 1 wt% samples. At this concentration, the mixtures are all apparently stable sols. However, the behavior of the second peak is similar to the cases for the 10 wt% samples, suggesting interparticle correlation is the strongest at  $\text{pH} = 4.5$ . As pointed out above, the surface charges are still negative at this  $\text{pH}$  value, and there are not enough  $\text{Na}^+$  ions on the surfaces to cause coagulation (Allen and Matijevic 1969; Milonjic 1992). Thus, this strengthening of interparticle correlation at  $\text{pH} = 4.5$  for the 1 wt% samples, which no doubt is closely related to gelation at higher concentration, is caused by some yet unknown factors.

#### ACKNOWLEDGMENTS

This work was supported by Alberta Oil Sand Technology and Research Authority. The position of guest professorship for one of us (Y.K.) at the Center for Ceramics Research, Research Laboratory of Engineering Materials, Tokyo Institute of Technology, was supported by the Ministry of Education, Science, and Culture, Japan. We thank Dr. R. Schutte, Syncrude, Canada for drawing our attention to the references (Nikolov and Wasan 1992) and (Wasan et al. 1992) and Dr. Monkenbusch for providing the software "MUX" and "DEMUX".

#### REFERENCES

- Allen LH, Matijevic E. 1969. Stability of colloidal silica: I. Effect of simple electrolytes. *J Coll Interf Sci* 31:287–296.
- Barta L, Kooner ZS, Hepler LG, Roux-Dosgranges G, Grolier J-PE. 1989. Thermal and volumetric properties of chloroform + dimethylsulfoxide: thermodynamic analysis using the ideal associated solution model. *J Sol Chem* 18:663–673.
- Bhatia AB. 1984. On the zero wavenumber factors of binary associating mixtures. *Phys Chem Liq* 13:241–253.



- Brinker CJ, Scherer GN. 1990. Sol-gel Science—The physics and chemistry of sol-gel processing. San Diego:Academic Press 331p.
- Bunce J, Ramsay JDF. 1985. Small-angle neutron-scattering studies of silica sols in water at high temperatures. *J Chem Soc, Faraday Trans 1* 81:2845–2854.
- Costas M, Patterson DP. 1985. Heat capacities of water+organic-solvent mixtures. *J Chem Soc, Faraday Trans 1* 81:2381–2398.
- Dethelfson C, Sorensen PG, Hvidt Aa. 1984. Excess volumes of propanol-water mixtures at 5, 15 and 25°C. *J Sol Chem* 13:191–202.
- Everett DH. 1989. Basic principles of colloid science. London:Royal Society of Chemistry. 159p.
- Franks F, Desnoyers JE. 1985. Alcohol-water mixtures revisited. In:Franks F, editor. Water science reviews 1. London:Cambridge Univ. Press. 171–232.
- Groot RD. 1990. Recent theories on the electric double layer. In:Bloor DM, Wyn-Jones E, editors. The structure, dynamics, and equilibrium properties of colloidal systems. The Netherlands:Kluwer Academic Press; 801–812.
- Groot RD. 1991. On the equation of state of charged colloidal systems. *J Chem Phys* 94:5083–5089.
- Guinier A, Fournet G. 1955. Small-angle Scattering of X-rays. New York:John Wiley and Sons. 149–151.
- Handa YP, Zakrzewski M, Fairbridge C. 1992. Effect of restricted geometries on the structure and thermodynamic properties of ice. *J Phys Chem* 95:8594–8599.
- Matsuoka H, Tanaka H, Hashimoto T, Ise N. 1987. Elastic scattering from cubic lattice systems with paracrystalline distortion. *Phys Rev B* 36:1754–1765.
- Matsuoka H, Murai H, Ise N. 1988. “Ordered” structure in colloidal silica particle suspensions as studied by small-angle x-ray scattering. *Phys Rev B* 37:1368–1375.
- Milonjic SK. 1992. A relation between the amounts of sorbed alkali cations and the stability of colloidal silica. *Coll & Surfaces* 63:113–119.
- Monkenbusch M. 1991. DEMUXMUX: removal of multiple scattering from small-angle data. *J Appl Cryst* 24:955–958.
- Moonen JAHM. 1987. Small angle scattering of colloidal dispersions [Ph.D. thesis]. The Netherlands:Univ. Utrecht. 137p.
- Nikolov AD, Wasan DT. 1992. Dispersion stability due to structural contributions to the particle interaction as probed by thin liquid film dynamics. *Langmuir* 8:2985–2994.
- Penfold J, Ramsay JDF. 1985. Studies of electrical double-layer interactions in concentrated silica sols by small-angle neutron scattering. *J Chem Soc, Faraday Trans 1* 81:117–125.
- Ramsay JDF, Booth BO. 1983. Determination of structure in oxide sols and gels from neutron scattering and nitrogen adsorption measurements. *J Chem Soc, Faraday Trans 1* 79:173–184.
- Ramsay JDF, Avery RG, Benest L. 1983. Neutron-scattering studies of concentrated oxide sols. *Faraday Discuss, Chem Soc* 76:53–63.
- Schaefer D, Martin JE, Cannell D, Wiltzins P. 1984. Fractal geometry of colloidal aggregates. *Phys Rev Lett* 52:2371–2374.
- Schelten J, Schmatz W. 1980. Multi-Scattering treatment for small-angle scattering problems. *J Appl Cryst* 13:385–390.
- Shuin T. 1977. Small-angle x-ray scattering analysis of particle size distributions of colloidal SiO<sub>2</sub> sol. *Jpn J Appl Phys* 16:539–548.
- Sogami I, Ise N. 1984. On the electrostatic interaction in macroionic solutions. *J Chem Phys* 81:6320–6332.
- Valleau JP, Ivkov R, Torrie GM. 1991. Colloid stability: the forces between charged surfaces in an electrolyte. *J Chem Phys* 95:520–532.
- Vonk CG. 1975. A general computer program for the processing of small-angle x-ray scattering data. *J Appl Cryst* 8:340–341.
- Vonk CG. 1976. On two methods for determination of particle size distribution functions by means of small-angle x-ray scattering. *J Appl Cryst* 9:433–440.
- Vonk CG, Pijpers AP. 1981. The use of film methods in small-angle x-ray scattering. *J Appl Cryst* 14:8–16.
- Vonk CG. 1988. A reevaluation of film methods in x-ray scattering. *Rigaku J* 5:9–17.
- Wasan DT, Nikolov AD, Kralchevsky PA, Ivanov IB. 1992. Universality in film stratification due to colloid crystal formation. *Coll & Surfaces* 67:139–145.
- Xu Y, Koga Y, Watkinson AP. 1994. Pore size distribution of coals and chars from Western Canada. *Fuel* 73:1797–1801.
- Xu Y, Chan SP, Koga Y. Personal communication. Department of Chemistry. The University of British Columbia, Vancouver, B.C., Canada V6T 1Z1.
- Zerrouk R, Foissy A, Mercier R, Chevallier Y, Morawski J-C. 1990. Study of Ca<sup>2+</sup>-induced silica coagulation by small angle scattering. *J Coll Interf Sci* 139:20–29.

(Received 16 September 1994; accepted 14 July 1995; Ms. 2574)